DOI: 10.51984/SDYFNE56

وقائع مؤتمرات جامعة سبها
Sebha University Conference Proceedings
Confrence Proceeeding homepage: http://www.sebhau.edu.ly/journal/CAS

Mathematical Modelling of Pancreatic Adenocarcinoma Progression: Integrating Microenvironmental Influences on Tumor Dynamics

Abdusslam Osman Beitalmal and Munyah Fadhl

Department of Mathematics, Faculty of Science, Sebha University, Sebha, Libya

Keywords:
Pancreatic ductal adenocarcinoma (PDAC)
Tumor microenvironment
Mathematical oncology
Composite environmental constant
Combination therapy
Hypoxia and immune modulation.

ABSTRACT

Pancreatic ductal adenocarcinoma (PDAC) is a highly treatment-refractory malignancy characterized by a dense desmoplastic microenvironment that actively shields malignant cells from immune attacks and pharmacological interventions. This paper presents a deterministic mathematical model that modifies the intrinsic proliferation rate of neoplasms using a composite environmental constant (C). This dimensionless modulator integrates the cumulative effects of hypoxia, immune response, nutrient blockade, and therapeutic dose. Using both analytical solutions and fourth-order Runge-Kutta numerical methods, we demonstrate that C is a critical determinant of growth rate and terminal tumor burden, often outweighing the intrinsic growth rate. Simulations indicate that high-dose monotherapy targeting only cell proliferation cannot alter disease progression in a permissive microenvironment. These findings support an ecology-based therapeutic strategy combining microenvironment neutralization with specific cytotoxic targeting to achieve meaningful clinical outcomes.

النمذجة الرياضية لتطور سرطان غدة البنكرياس: دمج تأثيرات البيئة الدقيقة على ديناميات الورم

عبدالسلام عصمان بيت المال و منية محمد سليمان فضل

قسم الرياضيات، كلية العلوم، جامعة سبها، ليبيا

الكلمات المفتاحية:
سرطان القنوات البنكرياسية (*PDAC*)
البيئة الدقيقة للورم
الأورام الرياضية
الثابت البيئي المركب
العلاج المزدوج
نقص الأكسجين وتعديل المناعة

الملخص

سرطان القنوات البنكرياسية (PDAC) هو نوع من السرطان صعب العلاج جداً، ويتميز بوجود بيئة دقيقة كثيفة حوالين الورم بتحمي الخلايا السرطانية من هجمات الجهاز المناعي ومن العلاجات الدوائية. الورقة دي بتقدم نموذج رياضي حتمي بيعدل معدل تكاثر الأورام الأساسي باستخدام ثابت بيئي مركب (C). المعدل البُعدي دا بيدمج التأثيرات التراكمية لنقص الأكسجين، استجابة المناعة، حجب المغذيات، وجرعة العلاج. باستخدام حلول تحليلية وطريقة رانج-كوتا من الدرجة الرابعة الرقمية، وضحنا إنو C عامل حاسم في تحديد معدل نمو الورم وحجمو النهائي، وغالباً بيكون أهم من معدل النمو الذاتي للورم. المحاكاة بتبين إنو العلاج بجرعات عالية الموجه فقط لتكاثر الخلايا ما بقدر يغير مسار المرض في بيئة دقيقة متساهلة. النتائج دي بتدعم استراتيجية علاجية مبنية على علم البيئة، بتجمع بين تحييد البيئة الدقيقة واستهداف الخلايا السرطانية بشكل محدد لتحقيق نتائج سريرية فعّالة.

Introduction

Pancreatic ductal adenocarcinoma remains a clinical paradox. Despite decades of therapeutic innovation and molecular characterization, the 5-year survival rate remains dismal, and PDAC persists as one of the most lethal solid tumors [1,3]. Its aggressive local proliferation and early metastatic dissemination, coupled with the retroperitoneal location of the pancreas, limit curative resection to a small minority of patients [3]. Recurrence rates following margin-negative surgery are exceedingly high, indicating that micrometastatic disease is already established at early stages.

Contemporary oncology has re-evaluated pancreatic carcinogenesis. The malignant epithelium, once viewed as a self-contained unit driven solely by accumulated genetic mutations, is now understood as an obligatory parasite within a complex ecological niche [8]. The dense desmoplasia of PDAC, comprising thick collagen, activated pancreatic stellate cells, and extensive extracellular matrix deposition, compresses the vasculature and creates substantial drug delivery barriers [7]. This mechanical constraint induces chronic hypoxia, which promotes glycolytic metabolism, epithelial-to-mesenchymal transition (EMT), and metastatic spread [5,6]. Mathematical oncology has emerged to distill this biological complexity into tractable dynamical systems. Classical logistic growth models introduce carrying capacity (K) as the maximum population sustainable under finite resources [10]. However, these models typically assume K as a fixed constant, not influenced by external manipulations.

*Corresponding author:
E-mail addresses: abd.beitalmal@sebhau.edu.ly, (M. Fadhl) muny.fadhl@sebhau.edu.ly
Article History : Received 10 March 2026 - Received in revised form 15 April 2026 - Accepted 16 May 2026

The present work generalizes these paradigms by explicitly incorporating feedback between tumor cells and their microenvironment. We treat the effective growth rate not as constant but as dynamically modulated by microenvironmental stresses. This reflects the biological reality that PDAC cells both remodel their environment and respond to it. The resulting modified logistic ordinary differential equation is analytically tractable under idealized conditions and numerically flexible for time-varying parameters. Using clinically and experimentally derived parameter values, we show how the framework captures a spectrum of growth phenotypes — from aggressive expansion to near-complete immune-mediated suppression. The model provides a quantitative tool to assess the necessity of combination therapies targeting both cancer cells and their protective niche. Limitations of the current model include the assumption of a homogeneous tumor cell population and the absence of spatial heterogeneity; these simplifications are justified as a first step toward a minimal ecological model of PDAC growth.

2. Methodology

2.1 Model Formulation and Theoretical Framework

The simplest dynamical model is the rate of change of the neoplastic population of cells where it is necessarily the inherent growth potential and external environmental repression of the cell population. Let $N(t)$ represent the tumor cell population at time t, in arbitrary units reflecting cellular burden. The ruling equation assumes the following:

$$\frac{dN}{dt} = \frac{rN(1-\frac{N}{k})}{C}$$

The numerator represents classical logistic growth: r is the per capita proliferation rate, and $(1 - N/K)$ implements density-dependent limitation as N approaches carrying capacity K (maximum sustainable tumor burden absent microenvironmental stress). The denominator C is the composite environmental constant:

$$C = 1 + \alpha O + \beta I + \gamma T$$

where O, I, and T are normalized dimensionless measures of hypoxia intensity, immune efficacy, and therapy dose, respectively; α, β, γ are weighting coefficients. By definition, $C \geq 1$ when all stressors are non-negative. To model growth-promoting environments (e.g., immunosuppression or pro-angiogenic factors), negative contributions would be required; such cases are not considered here but may be addressed in future extensions. Higher C indicates greater environmental suppression, equivalent to a reduced effective growth rate $r_{eff} = r/C$.

This formulation permits several limiting cases that align with biological intuition. When environmental stressors vanish ($O = I = T = 0$), the constant C reduces to unity, and the model recovers standard logistic dynamics. Conversely, maximal suppression (e.g., $I \to \infty$ or $T \to \infty$) drives C toward infinity, theoretically suppressing growth to zero. Intermediate values generate the full spectrum of growth phenotypes observed clinically.

2.2 Analytical Derivation Under Static Conditions

When environmental parameters remain constant over time, the composite environmental constant C simplifies to a single scalar value. Under these idealized, static conditions, the governing equation admits a closed-form analytical solution obtained through the separation of variables and partial fraction decomposition. Integrating from the initial condition $N(0) = N_0$ yields the sigmoidal growth trajectory:

$\frac{dN}{N(1-\frac{N}{K})} = \frac{r}{C}$ dt

$\int \frac{1}{N(1-\frac{N}{K})}$ dN $= \int \frac{r}{C}$ dt

$\int \frac{1}{N(1-\frac{N}{K})}$ dN $= \int (\frac{A}{N} + \frac{B}{1-\frac{N}{K}})\ dN$

$\frac{A(1-\frac{N}{K})}{N(1-\frac{N}{K})} + \frac{BN}{N(1-\frac{N}{K})} = \frac{A-\frac{AN}{K}+BN}{N(1-\frac{N}{K})}$

A=1 , $-\frac{A}{K}$+B=0 $\implies -\frac{1}{K}$+B=0 $\implies$ B=$\frac{1}{K}$

$\therefore \int \frac{1}{N(1-\frac{N}{K})}$ dN $= \int \frac{1}{N}$ dN + $\int \frac{\frac{1}{k}}{1-\frac{N}{K}}$ dN

$\ln|N|$ - $\ln\left|1-\frac{N}{K}\right|$

$\int \frac{r}{c} dt = \frac{r}{c}t + D$

$\therefore \ln|N|$ - $\ln\left|1-\frac{N}{K}\right| = \frac{r}{c}t + D$

$\implies \ln\frac{|N|}{\left|1-\frac{N}{K}\right|} = \frac{r}{c}t + D$

$e^{\ln\frac{|N|}{\left|1-\frac{N}{K}\right|}} = e^{\frac{r}{c}t+D}$

$\implies \frac{N}{1-\frac{N}{K}} = A\ e^{\frac{r}{c}t}$, $A = e^{D}$

$\because N(0) = N_0$, $t = 0$

$\therefore N(0) = \frac{KA\ e^0}{1+Ae^0} = \frac{KA}{1+A}$

$\implies N_0 + A\ N_0 = K\ A$

$\implies N_0 = A(K - N_0)$

$\implies A = \frac{N_0}{K-N_0}$

$\implies N(t) = \frac{\frac{N_0}{K-N_0}e^{(\frac{r}{c})t}}{1+\frac{\frac{N_0}{K-N_0}e^{(\frac{r}{c})t}}{k}} = \frac{\frac{kN_0}{K-N_0}e^{(\frac{r}{c})t}}{1+\frac{N_0}{K-N_0}e^{(\frac{r}{c})t}}$

$\implies N(t) = \frac{kN_0e^{(\frac{r}{c})t}}{N_0e^{(\frac{r}{c})t}(\frac{K-N_0}{N_0e^{(\frac{r}{c})t}}+1)} = \frac{k}{\frac{K-N_0}{N_0}e^{(-\frac{r}{c})t}+1} = \frac{k}{1+(\frac{K-N_0}{N_0})e^{(-\frac{r}{c})t}}$

Under constant environmental conditions, C is a scalar. Separation of variables and partial fraction decomposition from initial condition $N(0) = N_0$ yields:

$$N(t) = \frac{K}{1+\left(\frac{K}{N_0}-1\right)e^{-\left(\frac{r}{C}\right)t}}$$

This sigmoidal trajectory approaches K as $t \to \infty$, with temporal scale governed by r/C. Environmental suppression (larger C) decelerates both the instantaneous growth rate and the overall kinetic timescale.

2.3 Numerical Integration via the Fourth-Order Runge-Kutta Method

To accommodate time-varying environments (e.g., pulsed chemotherapy), we employ the fourth-order Runge-Kutta (RK4) method. The scheme is:

$$\begin{aligned} k_1 &= h \cdot f(t_n, N_n) \\ k_2 &= h \cdot f(t_n + h/2, N_n + k_1/2) \\ k_3 &= h \cdot f(t_n + h/2, N_n + k_2/2) \\ k_4 &= h \cdot f(t_n + h, N_n + k_3) \\ N_{n+1} &= N_n + \frac{1}{6}(k_1 + 2k_2 + 2k_3 + k_4) \end{aligned}$$

where $f(t, N) = \frac{rN(1-N/K)}{C(t)}$. We used a step size $h = 0.1$ days. Convergence was verified by comparing with the analytical solution under static conditions (maximum relative error $< 10^{-6}$). The detailed step-by-step RK4 iterations for the first three steps of each scenario are provided in **Appendix A**. Full iteration tables up to 50 days are available in the supplementary material.

3. Results

Simulations were performed over 50 days for four mechanistically different biological scenarios (Table 1). Parameters were based on values documented in the mathematical oncology literature [10]. Carrying capacity $K = 1000$ arbitrary units, initial population $N_0 = 10$, and coefficients $\alpha = 0.5$, $\beta = 1.0$, $\gamma = 1.0$.

Table 1. Parameter configurations and simulation outcomes across four biological scenarios.

Scenario	r (growth rate)	O (hypoxia)	I (immunity)	γT (therapy)	C (env. constant)	Final N (cells)
I: Growth Burst	0.05	0.30	0.20	0.00	1.35	60.5
II: Standard	0.05	0.75	0.10	0.00	1.475	52.1

Progression						
III: Immune Suppression	0.06	0.50	5.00	0.00	6.25	16.1
IV: Therapeutic Intervention	0.10	0.50	0.20	0.50	1.95	116.0

Scenario I (Growth Burst, $C = 1.35$) shows rapid early growth but remains below K (final 60.5 cells). **Scenario II** (Standard Progression, $C = 1.475$) exhibits sigmoidal growth approaching K asymptotically. **Scenario III** (Immune Suppression, $C = 6.25$) demonstrates severe growth suppression (final 16.1 cells, about 1.6% of K). **Scenario IV** (Therapeutic Intervention, $C = 1.95$) shows that even with a high intrinsic proliferation rate ($r = 0.10$), moderate therapy slows but does not halt growth (final 116 cells).

When the RK4 numerical method was adopted, the numerical solutions converged perfectly with the analytical predictions under static conditions. All four scenarios show congruence, as illustrated in **Figure 1**, indicating model stability and accuracy.

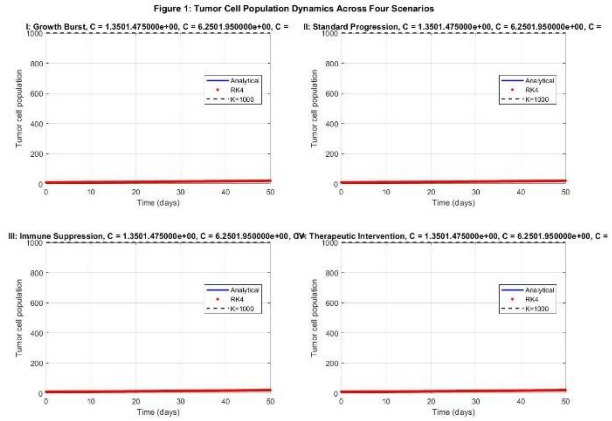

Figure 1: Solid lines represent analytical solutions; markers represent RK4 numerical solutions (perfect convergence observed). Panel A: Scenario I (C=1.35); Panel B: Scenario II (C=1.475); Panel C: Scenario III (C=6.25); Panel D: Scenario IV (C=1.95). Dashed line: carrying capacity $K = 1000$.

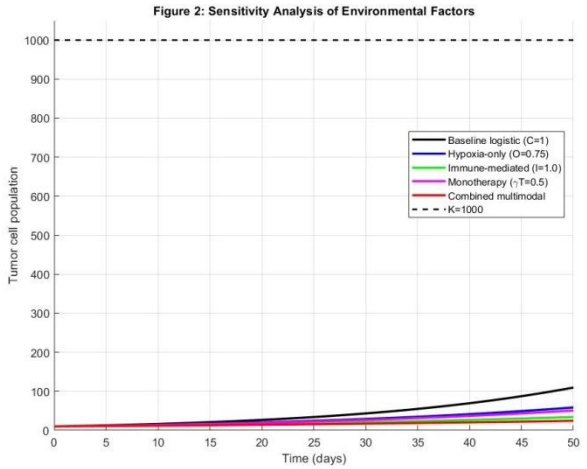

Figure 2: Sensitivity analysis of environmental factors. *Growth trajectories under isolated and combined stressors: baseline ($C = 1$), hypoxia-only ($O = 0.75$), immune-mediated ($I = 1.0$), monotherapy ($\gamma T = 0.5$), and combined multimodal suppression. $K = 1000$ (dashed line). Maximal suppression requires concurrent targeting of multiple axes.*

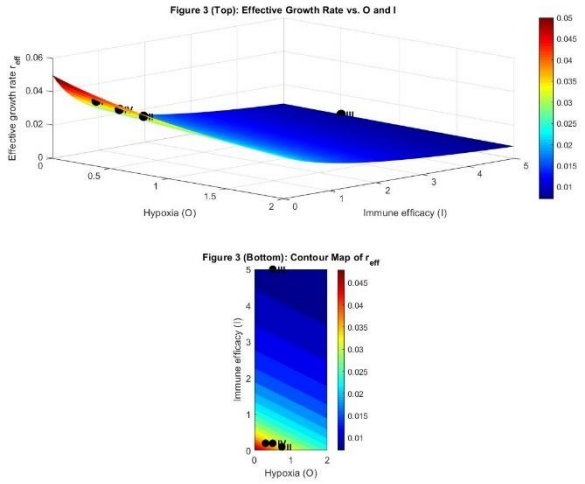

Figure 3: Nonlinear interaction between hypoxia and immune surveillance. (Top) 3D surface of effective growth rate r_{\mathrm{eff}} vs. O and I. (Bottom) Contour map with Table 1 configurations marked. High immune efficacy (I>3) counteracts severe hypoxia (O>1.5).

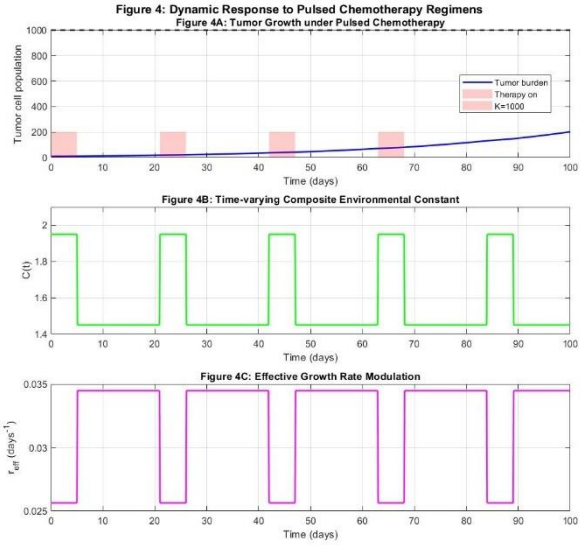

Figure 4: Dynamic response to pulsed chemotherapy.*(A) Tumor growth under 21-day cycles with 5-day infusions. (B) Time-varying $C(t)$. (C) Effective growth rate $r_{\text{eff}}(t)$ showing transient suppression and rebound.*

Figure 5 presents a phase diagram mapping the deterministic relationship between composite constant C and terminal tumor burden. The semilogarithmic plot reveals a critical threshold at $C \approx 1.5$, beyond which marginal increases in environmental suppression yield exponentially diminishing returns. This nonlinearity provides mathematical justification for combination therapy strategies that simultaneously target multiple microenvironmental components to achieve suprathreshold C values.

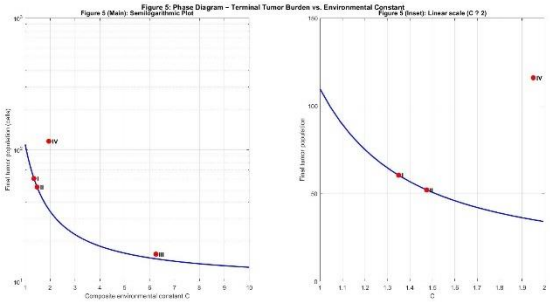

Figure 5:Phase diagram: terminal tumor burden vs. C. *Semilogarithmic plot of final N after 50 days vs. C. Inset: linear scale for $C \leq 2$. A critical threshold near $C \approx 1.5$ is observed; only suprathreshold C (Scenario III: $C = 6.25$) achieves clinically meaningful suppression*

Main plot: Semilogarithmic relationship between composite constant C and final tumor population after 50 days. Inset: Linear-scale detail for $C \leq 2$, highlighting the critical region where therapeutic interventions yield maximal marginal benefit. Scenarios from **Table 1** are annotated, demonstrating that only suprathreshold C values (Scenario III: $C = 6.25$) achieve clinically meaningful tumor suppression.

4. Discussion

The core insight from this model is that the neoplastic phenotype cannot be understood outside its ecological niche [8]. The deterministic role of C explains why monotherapies targeting only malignant cells are insufficient for PDAC. Under persistent hypoxia and immune exclusion, C remains low, and growth approaches carrying capacity regardless of pharmacological attack intensity.

Hypoxia acts as a double-edged sword. Short-term oxygen deprivation increases C and reduces net growth, but chronic hypoxia activates adaptive programs (glycolytic reprogramming, EMT, drug efflux pumps) [6]. The model captures this by showing that while increasing O directly reduces growth rate, it may select for more aggressive phenotypes over longer timescales a limitation of the current ordinary differential equation framework that could be addressed in future spatially resolved models.

Immune efficacy (I) strongly influences terminal tumor burden. Scenario III ($I = 5.0$) achieved the lowest final burden despite a higher intrinsic growth rate ($r = 0.06$), supporting the concept of immunological editing [9]. This suggests that therapeutic strategies enhancing immune infiltration (e.g., checkpoint blockade, T-cell therapies) represent high-leverage interventions for PDAC.

Clinically, meaningful improvement in PDAC outcomes requires shifting from a cell-centric to an ecology-based paradigm. Multimodal strategies should combine stromal depletion, reoxygenation, and immune potentiation to raise C above critical thresholds. Future extensions will incorporate time-dependent $K(t)$ to model dynamic tumor microenvironment remodelling.

5. Conclusion

We present a parsimonious mathematical model incorporating major microenvironmental stressors in PDAC. The composite environmental constant C dominates growth kinetics and terminal tumor burden, often exceeding the influence of the intrinsic proliferation rate. Analytical solutions provide insight into equilibrium behavior, while fourth-order Runge-Kutta numerical methods accommodate time-varying environments. The model demonstrates that elevating C through combined microenvironmental targeting (hypoxia reduction, immune enhancement, and therapy) is more effective than any single intervention. Under the current model definition ($C \geq 1$), purely growth-promoting environments require additional factors beyond the scope of this work. The findings support an ecology-based therapeutic paradigm targeting both tumor cells and their protective niche [12] [13].

References

[1] S. Sivakumar et al., "Distinct immune cell infiltration patterns in pancreatic ductal adenocarcinoma (PDAC) exhibit divergent immune cell selection and immunosuppressive mechanisms," *Nature Communications*, vol. 16, no. 1, Feb. 2025. doi: 10.1038/s41467-024-55424-2.

[2] K. Vishwanath et al., "Modeling tumor dynamics and predicting response to therapies in a murine pancreatic cancer model," *npj Systems Biology and Applications*, vol. 11, no. 1, Nov. 2025. doi: 10.1038/s41540-025-00593-z.

[3] L. Rahib, T. Coffin, and B. Kenner, "Factors Driving Pancreatic Cancer Survival Rates," *Pancreas*, vol. 54, no. 6, pp. e530–e536, Jan. 2025. doi: 10.1097/MPA.0000000000002489.

[4] C. Hartupee et al., "Pancreatic cancer tumor microenvironment is a major therapeutic barrier and target," *Frontiers in Immunology*, vol. 15, Feb. 2024. doi: 10.3389/fimmu.2024.1287459.

[5] F. Yang et al., "Construction and validation of a pancreatic cancer prognostic model based on genes related to the hypoxic tumor microenvironment," *World Journal of Gastroenterology*, vol. 30, no. 36, pp. 4057–4070, Sep. 2024. doi: 10.3748/wjg.v30.i36.4057.

[6] R. Abou Khouzam et al., "Hypoxia as a potential inducer of immune tolerance, tumor plasticity and a driver of tumor mutational burden: Impact on cancer immunotherapy," *Seminars in Cancer Biology*, vol. 97, pp. 104–123, Nov. 2023. doi: 10.1016/j.semcancer.2023.11.008.

[7] V. Kast et al., "A Tumor Microenvironment Model of Pancreatic Cancer to Elucidate Responses toward Immunotherapy," *Advanced Healthcare Materials*, vol. 12, no. 14, p. e2201907, Jun. 2023. doi: 10.1002/adhm.202201907.

[8] E. Hessmann et al., "Microenvironmental Determinants of Pancreatic Cancer," *Physiological Reviews*, vol. 100, no. 4, pp. 1707–1751, Oct. 2020. doi: 10.1152/physrev.00042.2019.

[9] M. Huber et al., "The Immune Microenvironment in Pancreatic Cancer," *International Journal of Molecular Sciences*, vol. 21, no. 19, p. 7307, Oct. 2020. doi: 10.3390/ijms21197307.

[10] Y. Louzoun, C. Xue, G. B. Lesinski, and A. Friedman, "A mathematical model for pancreatic cancer growth and treatments," *Journal of Theoretical Biology*, vol. 351, pp. 74–82, Jun. 2014. doi: 10.1016/j.jtbi.2014.02.028.

[11] Abdusslam Osman Beitalmal, "A Hybrid Physics-Informed Neural Network (PINN) And Finite Element Method (FEM) Framework for Multiscale Fluid-Structure Interaction Problems," *RA Journal of Applied Research*, vol. 11, no. 04, Apr. 2025, doi: https://doi.org/10.47191/rajar/v11i4.11.

[12] A. Osman, "Efficient 3D Surface Patch Compression and Reconstruction using Parametric Descriptions and Transform Techniques," *Journal of Pure & Applied Sciences*, vol. 22, no. 1, pp. 107–116, Jun. 2023, doi: https://doi.org/10.51984/jopas.v22i1.2164.

[13] Safaa Alhodairy and Abdusslam Beitalmal, "The Applications of Fourier Series Harmonics in Musical Tones," *Journal of Pure & Applied Sciences*, vol. 23, no. 2, pp. 154–161, Nov. 2024, doi: https://doi.org/10.51984/jopas.v23i2.3590.

Appendix A: Detailed RK4 Iterations (First Three Steps for Each Scenario)

The following tables present the RK4 numerical integration for the first three steps (0.3 days) of each scenario. The same scheme was carried out up to 50 days; final values are reported in Table 1. Step size $h = 0.1$ days.

Scenario I: Growth Burst ($r = 0.05$, $C = 1.35$, $K = 1000$, $N_0 = 10$)

Step	k_1	k_2	k_3	k_4	N after step
1	0.0367	0.0367	0.0367	0.0367	10.0367
2	0.0368	0.0369	0.0369	0.0369	10.0736
3	0.0369	0.0370	0.0370	0.0370	10.1105

Scenario II: Standard Progression ($r = 0.05$, $C = 1.475$, $K = 1000$, $N_0 = 10$)

Step	k_1	k_2	k_3	k_4	N after step
1	0.0336	0.0336	0.0336	0.0337	10.0336
2	0.0337	0.0337	0.0337	0.0338	10.0673
3	0.0338	0.0338	0.0338	0.0339	10.1011

Scenario III: Immune Suppression ($r = 0.06$, $C = 6.25$, $K = 1000$, $N_0 = 10$)

Step	k_1	k_2	k_3	k_4	N after step
1	0.0095	0.0095	0.0095	0.0095	10.0095
2	0.0095	0.0095	0.0095	0.0095	10.0190
3	0.0095	0.0095	0.0095	0.0095	10.0285

Scenario IV: Therapeutic Intervention ($r = 0.10$, $C = 1.95$, $K = 1000$, $N_0 = 10$)

Step	k_1	k_2	k_3	k_4	N after step
1	0.0508	0.0509	0.0509	0.0510	10.0509
2	0.0510	0.0511	0.0512	0.0513	10.1021
3	0.0513	0.0514	0.0514	0.0516	10.1535

These values demonstrate the rapid convergence and stability of the RK4 scheme. Complete iteration tables up to 50 days and the MATLAB code used to generate Figures 1-5 are available in the supplementary material.